

**Broadband dielectric measurement & simulation of e-field curing systems**

Parker, Nyle ; Cuenca, J; Gumbleton, R; Dimitriou, Athanasios; Ormondroyd, Graham; Slocombe, Daniel

Timber 2018

Published: 26/06/2018

Peer reviewed version

[Cyswllt i'r cyhoeddiad / Link to publication](#)

Dyfyniad o'r fersiwn a gyhoeddwyd / Citation for published version (APA):

Parker, N., Cuenca, J., Gumbleton, R., Dimitriou, A., Ormondroyd, G., & Slocombe, D. (2018). Broadband dielectric measurement & simulation of e-field curing systems. In M. Spear (Ed.), *Timber 2018* (pp. 89-98).

Hawliau Cyffredinol / General rights

Copyright and moral rights for the publications made accessible in the public portal are retained by the authors and/or other copyright owners and it is a condition of accessing publications that users recognise and abide by the legal requirements associated with these rights.

- Users may download and print one copy of any publication from the public portal for the purpose of private study or research.
- You may not further distribute the material or use it for any profit-making activity or commercial gain
- You may freely distribute the URL identifying the publication in the public portal ?

Take down policy

If you believe that this document breaches copyright please contact us providing details, and we will remove access to the work immediately and investigate your claim.

BROADBAND DIELECTRIC MEASUREMENT & SIMULATION OF E-FIELD CURING SYSTEM

N. Parker¹, J. Cuenca¹, R. Gumbleton¹, A. Dimitrio², G. Ormondroyd², D. R. Slocombe¹

¹Cardiff University, Queen's Buildings, 14-17 The Parade CF24 3AA, Cardiff, UK

²BioComposites Centre, Bangor University, Deniol Rd, Bangor, LL57 2UW

SUMMARY

Broadband temperature dependent dielectric measurements of Polyvinyl alcohol have been taken for a frequency range of 100 MHz – 10 GHz. A numerical model of a high voltage capacitive applicator has been used to demonstrate heating uniformity of such a system.

KEYWORDS: (RF, curing, dielectric, measurement, conductivity)

INTRODUCTION

RF curing is used by the timber industry in many applications, such as multi-timber lamination (Pizzi, 2010). These are commonly known as, 'Glulams' which are used for structural elements in construction. Application of RF readily heats the adhesive agent causing it to cure rapidly while having minimal affect upon the timber. This is due to the large difference in dielectric loss between the timber (low loss) and the adhesive (high loss). When this technique is used in conjunction with pressing, a uniform well bonded laminate is formed. The complex dielectric constant is very important to an RF designer, as it shows whether a material is suitable for curing from an RF perspective.

Conventional methods ultimately rely upon convection/conduction to raise the adhesive to the desired temperature. This requires the total component to be raised to the required curing temperature. RF avoids the problems associated with a hot press, which must combat the low thermal conductivity of the timber (Mehdizadeh, 2015). RF allows for volumetric heating of the adhesive due to its dielectric properties.

Industry makes use of a wide variety of adhesives, which come in many variations. For this simulation, PVA was chosen as a baseline to demonstrate how dielectric measurements of the adhesive can be used to create an accurate numerical model. PVA is a semi crystalline polymer which contains the presence of OH groups and the hydrogen bond formation (Rajeswari, 2011). This paper will be using a generic PVA & water premix, it will be baked to remove the water content.

RF can be defined as the frequency range of 3 KHz – 300 MHz. The application of a high voltage, high frequency electric field to a lossy dielectric such as a water & PVA solution result in rapid heating due to the polarisation of the electric dipoles. (Tang, 2015) Polar molecules such as found in water, will continuously try to realign with an applied AC electric field. Alternative to this mechanism is ionic heating where the friction due to oscillating ions causes heating.

DIELECTRIC THEORY

THEORY

The complex permittivity is divided into two portions, the real part is related to the phase and is commonly called the dielectric constant. The imaginary accounts for the energy losses within a material and is aptly named the dielectric loss factor.

$$\epsilon^* = \epsilon' - j \epsilon'' \quad \text{Equation 1}$$

Where,

ϵ' is Dielectric Constant, ϵ'' is Dielectric Loss

$$\vec{J} = (\sigma + \epsilon_0 \epsilon'' \omega) \vec{E} + j \epsilon_0 \epsilon' \omega \vec{E} \quad \text{Equation 2}$$

Where,

σ	DC or Free Charge Conductivity	(S/m)
ϵ_0	Permittivity of free space	(F/m)
ϵ'	Dielectric Constant	
ϵ''	Dissipation Factor	
ω	Angular Frequency	(rad/s)
\vec{E}	Electric Field	(V/m)

$$P = \epsilon_0 \epsilon'' \omega |E|^2 \quad \text{Equation 3}$$

Both temperature and frequency play a contributing role to the currents generated when an AC electric field is applied to a dielectric such as PVA or Pine Wood. $P = \epsilon_0 \epsilon'' \omega |E|^2$

Equation 3 indicates that the dielectric loss sets the amount of power which can be deposited into the dielectric material.

EXPERIMENTAL

Broadband Dielectric Probe Measurement Technique

To determine the complex dielectric properties of the adhesive & timber for a broad frequency range, a broadband coaxial probe was used. The material load placed at the open boundary of a coaxial transmission line. This causes it to perturb the electric field at the open junction of the probe.

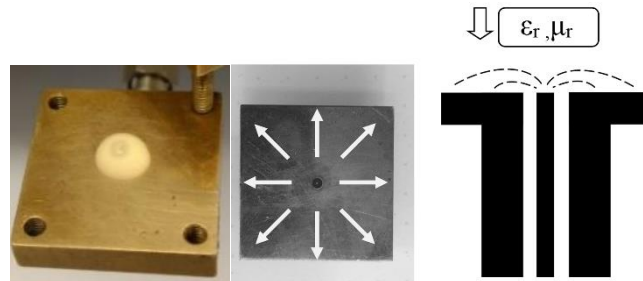


Figure 1 a) Physical probe viewed from above, the Electric Field propagates from the centre conductor to each boundary of the probe edge. b) Cross section of the probe, showing the Electric field lines from the centre conductor to the ground plate. c) Loaded Probe

An approximate expression for the measured complex permittivity is defined by (Cuenca, 2015) where full details for the measurement technique can be found.

Error! Reference source not found. Equation 4

Where,

$\epsilon_{r,eff}$	Relative Effective Permittivity	
ω ,	Angular Frequency	(rad/s)
C_0 ,	Capacitance (probe terminated by free space)	F
Z_0 ,	System Impedance (50)	Ω
Γ_L ,	Load Reflection Coefficient	
Γ_a ,	Air Reflection Coefficient	

The dielectric probe is connected to a Vector Network Analyser (VNA), which has been calibrated for a frequency range of 100 MHz – 10 GHz. The complex dielectric properties of both the adhesive and timber will be obtained for this range. As the adhesive cures the complex dielectric constant will change, the material will become less lossy and therefore a limit is put on the max temperature for a given input voltage.

The complex permittivity has been measured for two different temperatures, 30°C & 60°C respectively. Two temperature sensors are connected to the body of the probe to measure the temperature. This was achieved by placing the test fixture into a MEMMERT lab oven.

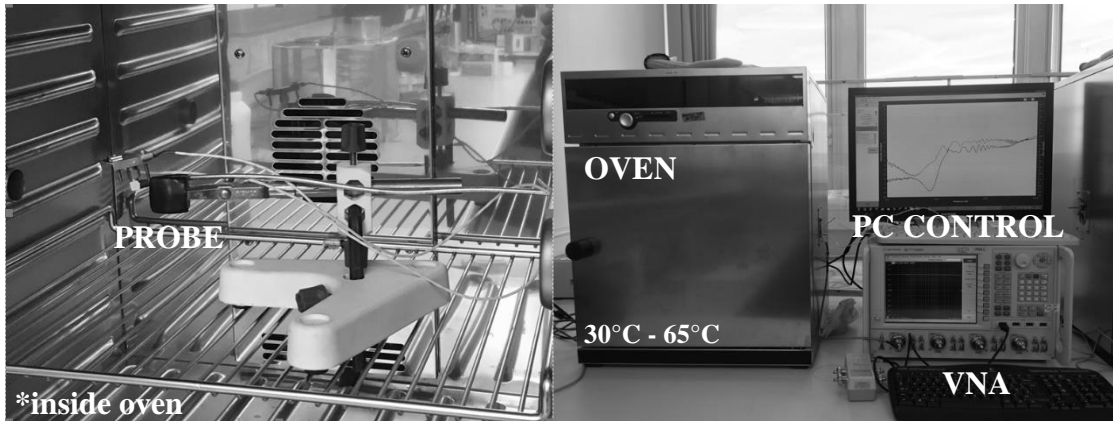


Figure 2 – Probe inside oven, preheated to desired temp before sample is added.

Electrical Conductivity

$$\sigma_T = \sigma_{dc} + \sigma_{ac} \quad \text{Equation 5}$$

The total conductivity is composed of a dc and ac element as shown below.

$$\sigma_T = \omega\epsilon_0\epsilon'' + j\omega\epsilon_0(\epsilon'' - \epsilon_\infty) \quad \text{Equation 6}$$

Due to the frequency of operation, the dc conductivity component is the desired parameter.

Experiment 1,2 – Time Dependent Complex Permittivity Measurement of PVA at 30°C, 60°C

This measurement was taken to determine the change in dielectric properties of the PVA as it cures in time, where water is being evaporated off. The oven is preheated to 30°C, then a small sample of the adhesive is applied to the dielectric probe end. The VNA is instructed to sample every 2s where the S11 data is converted into the complex permittivity values. Maintaining a constant temperature will show the change in complex dielectric constant as a function of time for the measured frequency range. Data is recorded until the water have been driven off as indicated by the loss in Debye characteristic at the higher frequency range. The measurement is then repeated for 60°C.

Experiment 3 Dielectric Measurement Temperature Ramp Results

Complex dielectric permittivity for 5 samples is measured across a temperature ramp of 30 °C - 65 °C. The system is first calibrated then the sample added to the probe, the oven is then set.

RESULTS AND DISCUSSION

Experiment 1

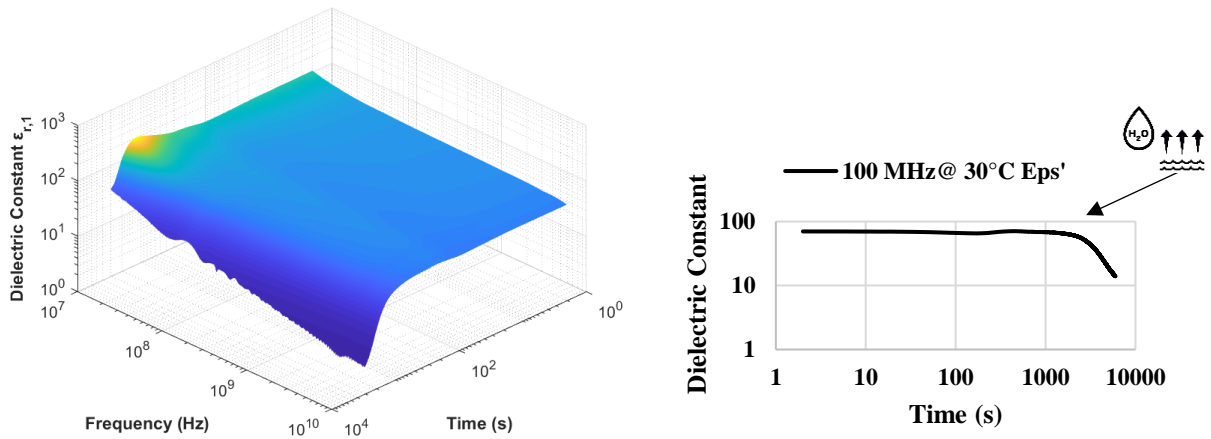


Figure 3 – a) Change in Dielectric Constant of PVA until it cures in time for a constant temperature of 30°C. b) Dielectric constant at 30°C for $f=100$ MHz

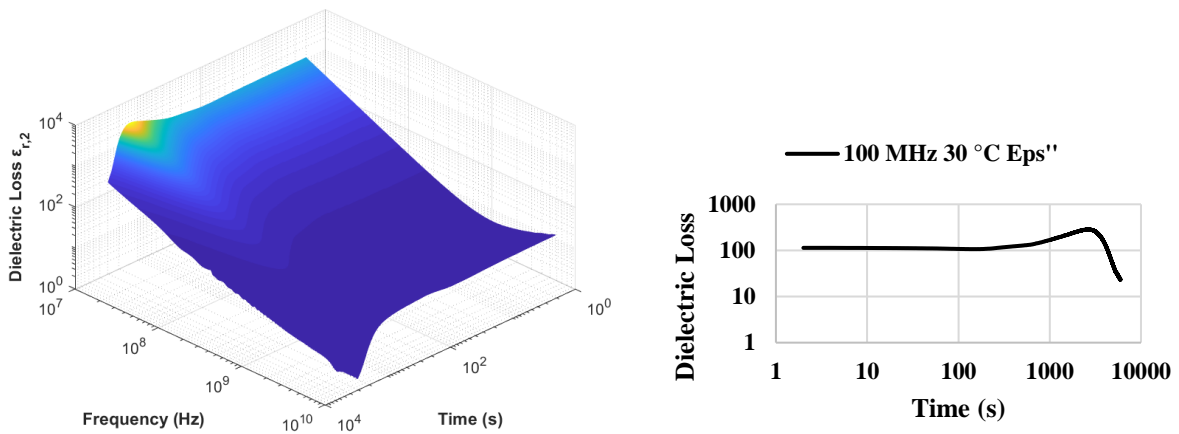


Figure 4 – a) Change in Dielectric Loss of PVA until it cures in time for a constant temperature of 30°C. b) Dielectric Loss at 30°C for $f=100$ MHz

The test fixture was maintained at a constant 30°C where the PVA was left to cure, with the instruments sampling every 2 seconds. Figure 3 (a) shows the relationship between the dielectric constant as time progresses as a function of frequency. As time progresses the dielectric constant is gradually decreasing, then at the knee point rapid decrease is observed.

Experiment 2

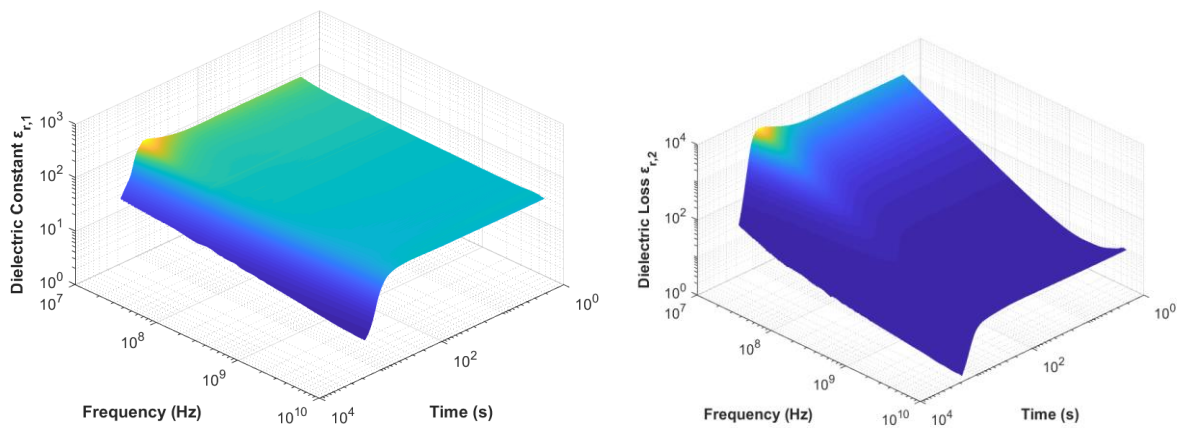


Figure 5 – a) Change in Dielectric Constant of PVA until it cures in time for a constant temperature of 60°C. b) Dielectric Loss

The results shown by **Error! Reference source not found.**, that after curing the Debye relaxation contributed by the water has been removed. It was this metric which was chosen to define the time where the measurement would end. It should be noted that there may be a small amount of water still present, as it was not baked for an extended period.

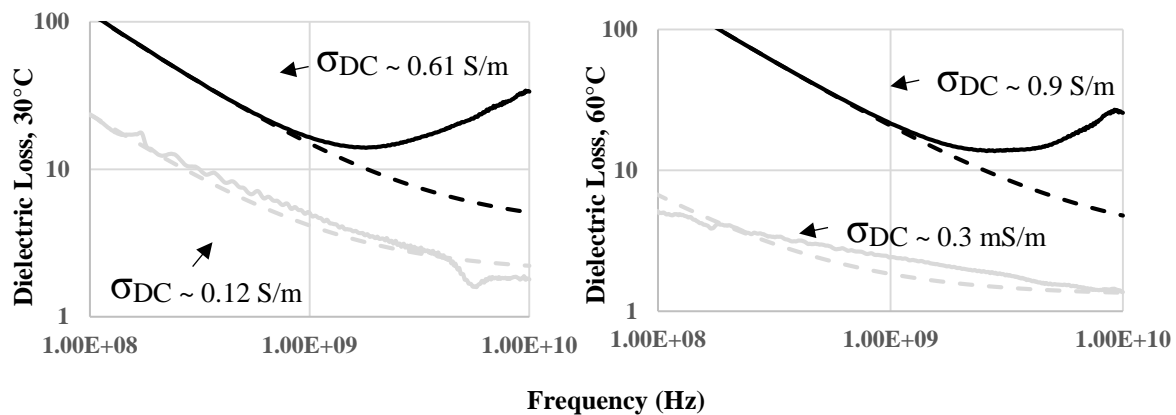


Figure 6-a) Dielectric loss for **uncured** & cured at 30°C, b) Dielectric loss for **uncured** & cured at 60°C.

This measurement observed the change in dielectric at a constant temperature in time for the frequency range shown in Figure 6. In b) the dielectric loss is greatly reduced as time passes. A cured value of 0.3mS/m for the 60°C is observed. Experiment 3 Dielectric Measurement Temperature Ramp Results

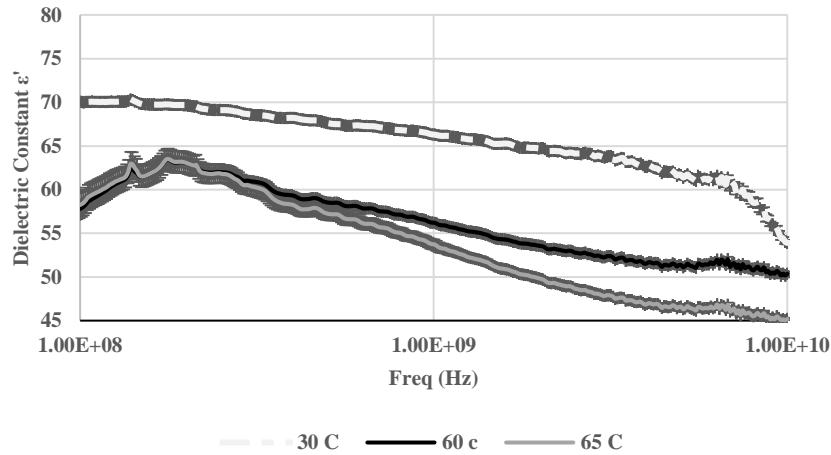


Figure 7 - Dielectric Constant vs Frequency for 3 temperatures

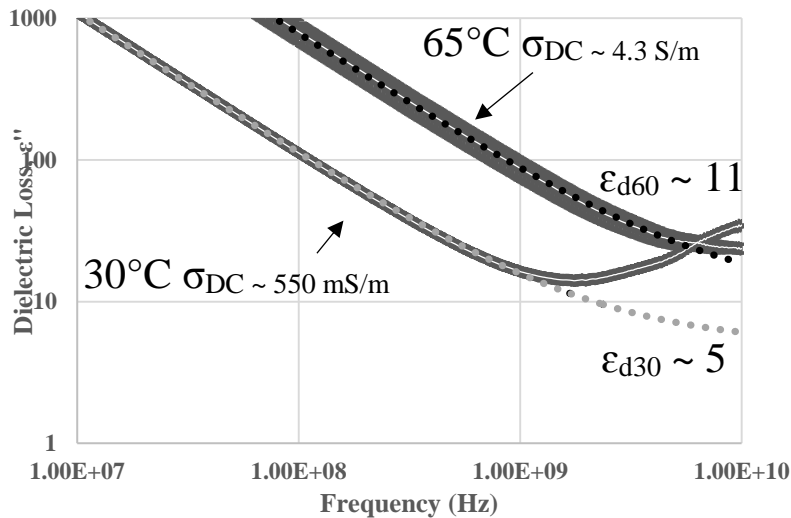


Figure 8 - Dielectric Loss & DC fitted conductivity. Standard error plotted for $n=5$.

Figure 8 shows the average dielectric loss of 5 samples for 2 temperatures. With increasing temperature, increasing electrical conductivity is observed. It must be noted that the result here is also influenced by the PVA curing in time. The σ_{DC} has increased from $\sim 550\text{mS/m}$ to 4.3S/m for a temp of 60°C . The conductivity (σ) of the each samples is found to increase linearly with frequency.

RF Simulation at 100 MHz

Earlier the complex dielectric properties of the materials were determined for a broad frequency range. A simulation of the RF will now be demonstrated for a frequency of 100 MHz, where the adhesive exhibits a high loss characteristic.

Table 1: Dielectric Properties of sample materials at 100 MHz

	ϵ_1	ϵ_2	σ_{DC}
30°C PVA Uncured	70.02	113.74	0.61 S/m
60°C PVA Uncured		179.14	0.90 S/m
Pine Wood	2.9	0.85	0.64 mS/m

The Arrhenius fit for σ_{DC} at 100 MHz valid for a temperature range of 30 °C to 65 °C.

$$\sigma(T) = \sigma_0 \exp\left(\frac{-E_a}{k_B T}\right) \quad \text{Equation 7}$$

Where,

- σ_{DC} , DC Electrical Conductivity, S/m
- σ_0 , Pre-exponential DC Electrical Conductivity, S/m
- E_a , Activation Energy, eV
- k_B , Boltzmann Constant, J/K
- T , Temperature, K

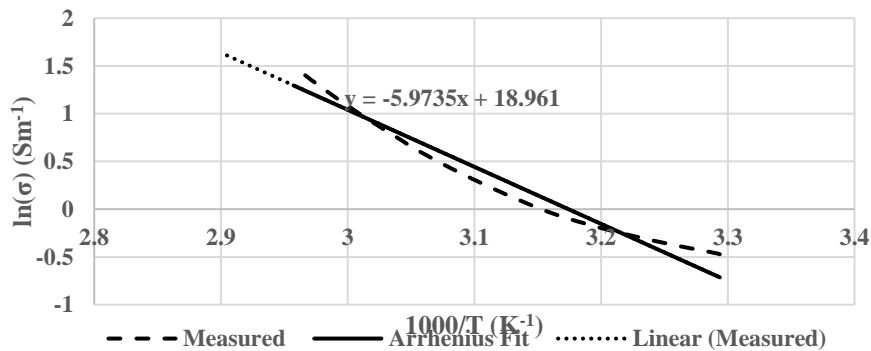


Figure 9 – Temperature (K^{-1}) dependent conductivity (Sm^{-1}) for PVA

Parallel Plate RF Applicator

This simulation will demonstrate the uniformity of the electric fields created by a capacitive applicator such as is commonly used in industry.

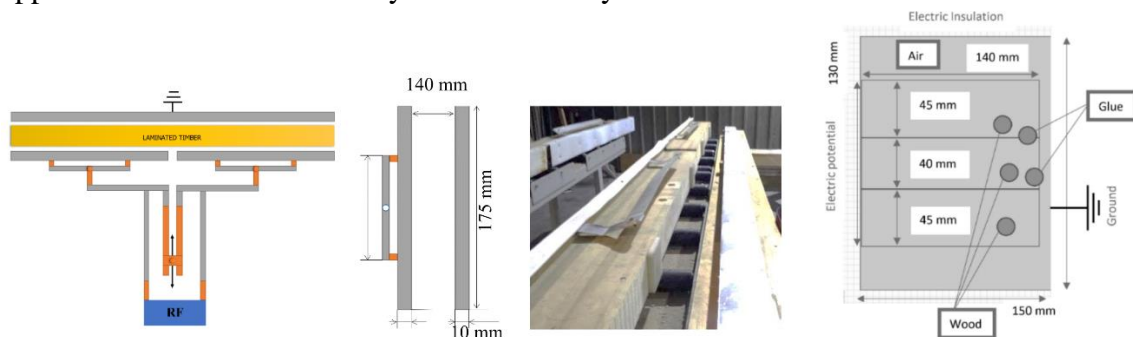


Figure 10 – a) Diagram of Physical System b) Photo of loaded system b) Simulation geometry

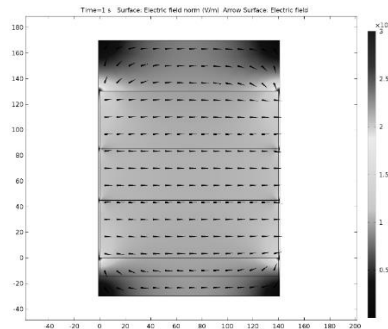


Figure 11 – **a**) Cross Section of Simplified Capacitive Applicator (Parker, 2017). **b**) E-Field Simulation for 100 MHz, 15kV.

Earlier work involved modelling a Glulam high voltage capacitive applicator, of which a cross section is shown in

Figure 11 (Parker, 2017). The model consists of a high voltage electrode to the far left, then the timber is stacked perpendicular to this plane with two glue lines used. At the far right is the ground plate. Future work will develop a model of electrical conductivity which considers both time and temperature simultaneously.

CONCLUSIONS

Broadband dielectric measurements of generic mix of PVA/Water were taken as a function of temperature. The results clearly showed that as time progressed that the water was being driven off, which resulted in the decay of the Debye response which water exhibits due to its highly polar nature at higher frequency. COMSOL was used to demonstrate the uniform electric field which can be generated by a parallel plate capacitive applicator, such as that commonly used for Glulam beams. Further work requires the complex dielectric properties to be recorded for a series of temperature vs time ramps.

ACKNOWLEDGEMENT

Lead & 3rd author would like to thank EPSRC and Renishaw Plc for their sponsorship.

REFERENCES

- Cuenca, J. e. (2015). Investigating the Broadband Microwave Absorption. *IEEE TRANSACTIONS ON MICROWAVE THEORY AND TECHNIQUES*, 4110-4118.
- International Telecommunication Union. (2005-09-08, 09 08). *Frequency Allocations*. Retrieved from Radio Club: <http://life.itu.int/radioclub/rr/art05.htm#Reg>
- Mehdizadeh, M. (2015). Electromagnetic joining with curable adhesives or joining agents. In M. Mehdizadeh, *Microwave/RF Applicators and Probes: for Material Heating, Sensing, and Plasma Generation* (pp. 272-273). London: Elsevier.
- Parker, N. (2017). Simulation of RF Fields for Wood Gluing Applications. *16th International Conference on Microwave and High Frequency Heating AMPERE*. Delft, The Netherlands: AMPERE.
- Pizzi, A. (2010). Glulam Beams. In A. Pizzi, *Wood Adhesives* (pp. 251-252). Leiden, Boston: CRC Press.
- Rajeswari, N. (2011). Conductivity and dielectric properties of polyvinyl alcohol–polyvinylpyrrolidone. *Journal of Non-Crystalline Solids*, 3751–3756.
- Tang, J. (2015). Dielectric Heating. In J. Tang, *Radio-Frequency Heating in Food Processing: Principles and Applications* (p. 5). Florida: CRC Press.